CMLS, Cell. Mol. Life Sci. 61 (2004) 1975–1984
1420-682X/04/151975-10
DOI 10.1007/s00018-004-4171-3

CMLS Cellular and Molecular Life Sciences

Research Article

Interaction of volkensin with HeLa cells: binding, uptake, intracellular localization, degradation and exocytosis

M. G. Battelli[a,*], S. Musiani[a], L. Buonamici[a], S. Santi[b], M. Riccio[c], N. M. Maraldi[c], T. Girbés[d] and F. Stirpe[a]

[a] Dipartimento di Patologia Sperimentale, Alma Mater Studiorum Università di Bologna, Via S. Giacomo 14, 40126 Bologna (Italy), Fax: +39 051 2094746, e-mail: mariagiulia.battelli@unibo.it
[b] Istituto per i Trapianti d'Organo e l'Immunocitologia, Consiglio Nazionale delle Ricerche, Sezione di Bologna, Bologna (Italy)
[c] Laboratorio di Biologia Cellulare e Microscopia Elettronica, Istituto Ortopedico Rizzoli, Bologna (Italy)
[d] Departamento de Bioquímica, Biología Molecular y Fisiología, Facultad de Ciencias Universidad de Valladolid, 47005 Valladolid (Spain)

Received 21 April 2004; received after revision 26 May 2004; accepted 9 June 2004

Abstract. Among two-chain ribosome-inactivating proteins (RIPs), volkensin is the most toxic to cells and animals, and is retrogradely axonally transported in the rat central nervous system, being an effective suicide transport agent. Here we studied the binding, endocytosis, intracellular routeing, degradation and exocytosis of this RIP. The interaction of volkensin with HeLa cells was compared to that of nigrin b, as an example of a type 2 RIP with low toxicity, and of ricin, as a reference toxin. Nigrin b and volkensin bound to cells with comparable affinity (approx. 10^{-10} M) and had a similar number of binding sites (2×10^5/cell), two-log lower than that reported for ricin. The cellular uptake of volkensin was lower than that reported for nigrin b and ricin. Confocal microscopy showed the rapid localization of volkensin in the Golgi stacks with a perinuclear localization similar to that of ricin, while nigrin b was distributed between cytoplasmic dots and the Golgi compartment. Consistently, brefeldin A, which disrupts the Golgi apparatus, protected cells from the inhibition of protein synthesis by volkensin or ricin, whereas it was ineffective in the case of nigrin b. Of the cell-released RIPs, 57% of volkensin and only 5% of ricin were active, whilst exocytosed nigrin b was totally inactive. Despite the low binding to, and uptake by, cells, the high cytotoxicity of volkensin may depend on (i) routeing to the Golgi apparatus, (ii) the low level of degradation, (iii) rapid recycling and (iv) the high percentage of active toxin remaining after exocytosis.

Key words. Intracellular routeing; nigrin b; ribosome-inactivating protein; ricin; volkensin.

Ribosome-inactivating proteins (RIPs) [reviewed in refs 1–4] from plants are characterized by an N-glycosidase activity, which removes a specific adenine residue (A_{4324} in rat liver rRNA) from eukaryotic rRNAs [5]. This depurination results in an irreversible alteration of the ribosomal proteo-synthetic machinery [6] with consequent cell death [7]. RIPs also depurinate DNA, and thus the denomination, adenine polynucleotide glycosylase, has been proposed for them [8].

RIPs are classically divided into type 1, single-chain proteins with enzymatic activity, and type 2, two-chain proteins consisting of an A chain similar to type 1 RIPs, and a B chain with lectin properties. A type 3 group of RIPs was also proposed recently, and under discussion is whether it should comprise two RIPs, JIP60 from barley [9] and b32 from maize, [10] or should be limited to the latter RIP only [2].

* Corresponding author.

Type 2 RIPs include some potent toxins, namely abrin, modeccin, ricin, viscumin and volkensin. Volkensin, from the Passifloraceae *Adenia volkensii*, is the most powerful of these [reviewed in ref. 11], with an LD_{50} of 1.7 µg/kg for mice, approximately 1/5 that of ricin, and 50–60 ng/kg for rats [12]. It also has the highest cytotoxicity, inhibiting protein synthesis by HeLa cells with an IC_{50} (concentration giving 50% inhibition) of 0.3 pM, approximately 1/3 that of ricin. Volkensin is also more toxic than ricin to nervous cells [13].

Toxic type 2 RIPs, like other lectins, are retrogradely transported along axons, and have been used to produce selective lesions in the nervous system by a technique termed 'molecular neurosurgery'. Modeccin and volkensin are the only toxins that are retrogradely transported not only along peripheral nerves, but also in the central nervous system, and for this property volkensin has been used in a variety of experiments [reviewed in ref. 14].

The toxicity of type 2 RIPs has been attributed to their structure: their B chains bind to sugar residues on the membrane of most cells, thus allowing and helping the entry of the A chains, which kill the cells through their enzymatic activity [reviewed in ref. 1]. Ricin, however, also enters macrophage and liver sinusoidal cells through an additional and alternative mechanism, through the mannose receptors of these cells, which bind the mannose residues present in the ricin molecule [15–17].

All type 2 RIPs were thought to be toxins, although a *Ricinus* agglutinin (RCA 120) was known which is a tetramer consisting of two A chains and two B chains with the same properties as the corresponding chains of ricin, but is much less toxic [reviewed in ref. 1]. During the last decade other lectins were found in *Cinnamomum*, *Eranthis*, *Iris*, *Momordica*, *Polygonatum* and *Sambucus* [reviewed in ref. 3], which are type 2 RIPs, with similar structure, and the same enzymatic and lectinic properties as ricin and related toxins. However, compared with toxic type 2 RIPs, they have a some thousandfold lower toxicity, similar to that of type 1 RIPs [reviewed in ref. 11].

The reasons for the different toxicity of toxic and nontoxic type 2 RIPs [reviewed in refs 3, 18], as well as for the differences in the potency of toxic type 2 RIPs are largely unknown. These differences cannot be explained by diversity in the catalytic activity of the A chains, which all efficiently inhibit cell-free protein synthesis. They could, rather, be due to differences between their B chains [19], which mediate the interaction with cells, in particular (i) binding to the cell membrane, (ii) the uptake by cells, (iii) the intracellular routeing, (iv) the degree of degradation and (v) the exocytosis of the toxin by cells.

The mechanism of entry and intracellular routeing of ricin has been extensively studied. This RIP binds to the terminal galactose or N-acetylgalactosamine residues of glycans largely exposed by glycoproteins and glycolipids of the cell surface [20]. After binding, ricin is taken up by cells either via a clathrin-dependent or a clathrin-independent pathway [reviewed in ref. 21]. Most of the internalized ricin is routed from the endosomal compartment to lysosomes, while a small fraction (only 5%) reaches the trans-Golgi network (TGN) [22]. The transport of ricin through the Golgi apparatus was suggested to be a crucial event in the cytotoxicity of this RIP [23]. Consistently, treatment of cells with brefeldin A (BFA), which disrupts the Golgi stack, strongly reduced the cytotoxicity of ricin [24, 25]. Afterwards (i) ricin reaches the endoplasmic reticulum (ER) by using the retrograde transport system of proteins recycling from the TGN to the ER compartment, (ii) the disulphide bridge between the A and B chain is reduced and (iii) the A chain enters the cytosol through the translocation path that mediates the routeing of misfolded proteins [reviewed in ref. 26].

Little information is available about the binding to, and the endocytosis by, cells of the less toxic type 2 RIPs. Battelli et al. [27] studied the binding to, and the internalization by, HeLa cells of nigrin b and compared it to ricin. Both RIPs initially followed the same pathways, binding to receptors on the cell membrane and reaching an endosomic compartment. From this point onward, nigrin b was recycled back to the plasma membrane into the lysosomal compartment and was expelled from cells, without apparently entering the TGN as ricin does. These results led to the suggestion that nigrin b has a low cytotoxicity because the majority of the RIP was degraded by cells and its intracellular routeing did not include passage through the TGN. A very low binding to the cell membrane was associated with a low cytotoxicity in the case of IRA, a type 2 RIP from *Iris*, which has an IC_{50} for HeLa cells of 1.34×10^{-7} M [28]. Also in the case of ebulin l, one of the type 2 RIPs from *Sambucus*, the negligible cytotoxicity (IC_{50} for HeLa cells 6.2×10^{-8} M [29]) was attributed to a reduced affinity of its lectin B chain for galactosides compared to the ricin B chain [30].

Nothing is known about the mechanism of entry into cells and intracellular routeing of volkensin. In previous studies, attempts were made to elucidate the intracellular fate of modeccin, a type 2 RIP from *A. digitata*, a plant belonging to the same family, Passifloraceae, as *A. volkensii*. After binding to the cell membrane, modeccin enters the cytosol by two different routes [31]: a major one that requires endosomal acidification and a minor one that is activated by nigericin [32]. Moreover, Yoshida et al. [24] have shown that BFA blocks the toxicity to Vero and other cell lines of both modeccin and ricin, suggesting an involvement of the Golgi apparatus in the activity of these toxins.

The present investigation was undertaken to study the binding, endocytosis, intracellular routeing, degradation and exocytosis of volkensin. HeLa cells were used to study the interaction of volkensin with cells in compari-

son with nigrin b, as an example of a type 2 RIP with low toxicity, and ricin, as a reference toxin. The intracellular localization of these RIPs was analyzed by confocal microscopy on immunostained samples. Anti-RIP polyclonal rabbit antibodies recognized p-formaldehyde-fixed antigens and allowed the performance of indirect immunofluorescence. Compared with direct methods, this technique has the advantage of avoiding any modification of the molecule to be detected; on the other hand, this analysis is not quantitative. This work may contribute to clarifying the reasons for the different toxicity of type 2 RIPs.

Materials and methods

Materials

Nigrin b, ricin and volkensin were prepared as described by Girbés et al. [33], Nicolson et al. [34] and Stirpe et al. [12], respectively. The RIPs were labelled with ^{125}I with the Iodogen reagent as described by Fraker and Speck [35]. Rabbit anti-RIP polyclonal antibodies were prepared as previously described [36].

BFA, bovine serum albumin (BSA) and 1,4-diazobicyclo-[2.2.2]-octane were from Sigma (St. Louis, Mo.). L-[4,5-^{3}H]leucine (3.1 TBq/mmol) was supplied by Amersham Biosciences (Rainham, UK). Fluorescein isothiocyanate (FITC)-conjugated goat anti-rabbit IgG polyclonal antibodies were from ICN ImmunoBiologicals (Lisle, Ill.). Cy5-conjugated donkey anti-mouse IgG polyclonal antibodies were from Jackson ImmunoResearch (West Grove, Pa.). Mouse GM130 monoclonal antibody was from BD Transduction Laboratories (Heidelberg, Germany). Mowiol 4-88 was from Aldrich-Chemie (Steinheim, Germany). All culture reagents were supplied by Gibco (Grand Island, New York). All other reagents were obtained from Merck (Darmstadt, Germany) and Farmitalia Carlo Erba (Milan, Italy).

Analysis of volkensin and nigrin b binding to HeLa cells

HeLa cells were seeded in 24-well tissue culture plates (8×10^4 cells/well) in RPMI 1640 medium supplemented with 10% FCS and antibiotics (complete medium). After 24 h at 37 °C, cells were incubated at 0 °C for 1 h with scalar concentrations (3×10^{-9}–10^{-7} M, 10^6 cpm/well) of ^{125}I-volkensin or ^{125}I-nigrin b, washed five times with ice-cold phosphate-buffered saline (PBS) pH 7.5, and dissolved in 0.1 N KOH for 10 min at 37 °C. Parallel cultures were incubated in the same conditions in the presence of 0.1 M lactose to determine the non-specific binding of ^{125}I-RIP to the cell membrane. The cell-associated radioactivity was determined in a γ-counter and was referred to protein concentration, determined as previously described [37]. Cell number was calculated by linear regression analysis using a standard protein concentration curve of a known number of cells. The number of binding sites per cell and the K_d values were determined by Scatchard analysis [38].

Cell protein synthesis

HeLa cells were seeded in 24-well tissue culture plates (3×10^4 cells/well) in complete medium. After 18 h, cells were incubated at 37 °C for different times with nigrin b, ricin or volkensin (5×10^{-6} M) or for 90 min with scalar concentrations of RIP (from 10^{-8} to 10^{-5} M) in complete (nigrin b and volkensin) or in serum-free (ricin) medium. After washing once with complete medium, cells were incubated at 37 °C for 30 min with L-[4,5-^{3}H]leucine (18.3 TBq/well) in serum- and leucine-free medium. Protein synthesis was arrested with 20% trichloroacetic acid (TCA). Cells were washed three times with 5% TCA and dissolved with 0.1 N KOH. The radioactivity incorporated by cells was measured in a β-counter with a liquid scintillation cocktail for aqueous solution [39]. The time of exposure to RIPs required to inhibit cell protein synthesis by 50% was calculated by linear regression analysis.

To evaluate the effect of BFA on the inhibition of cell protein synthesis by RIPs, cells were pre-incubated for 1 h at 37 °C with the drug (5 µg/ml) and then exposed to RIPs for 1–2 h in the presence of BFA and pulsed with L-[4,5-^{3}H]leucine to determine cell protein synthesis, as described above.

Endocytosis and exocytosis

HeLa cells were seeded in 24-well tissue culture plates (10^5 cells/well) in complete medium 18 h before the experiments. Binding to, uptake and degradation of RIPs by cells were determined as described by Battelli et al. [40] with minor modifications.

To measure the uptake of volkensin, cells were incubated with ^{125}I-RIP (10^{-8} M, 10^6 cpm/well) at 37 °C for 15–180 min in Hepes-buffered complete medium. After washing once with ice-cold medium and twice with PBS, the cells were stripped for 30 min at 0 °C with 0.1 M glycine/HCl buffer, pH 2, containing 0.04 M NaCl, to evaluate the amount of membrane-associated toxin after the warm incubation. Cells were extracted at 37 °C for 10 min with 0.1 M KOH to measure the intracellular accumulation of the RIP. Parallel cultures were incubated at 0 °C and stripped as above as a measure of the progressive binding of volkensin to HeLa cells.

To evaluate the amount and activity of RIPs released after endocytosis, cells were pulsed for 1 h at 0 °C with ^{125}I-RIP (5×10^{-8} M, 10^6 cpm/well), in complete medium, to allow cell binding. The plates were washed three times with ice-cold medium and further incubated at 37 °C for 15–180 min in complete medium. The internalization of RIPs was stopped by placing the plates on ice. An aliquot

(100 µl) of cellular supernatant was adjusted to 10% TCA (w/v final concentration) and centrifuged at 1130 g for 20 min to determine the amount of radioactivity recovered in the acid-soluble and in pelleted fractions as a measure of the degraded and undegraded exocytosed toxins, respectively. The remaining supernatant was collected to determine RIP activity by measuring the inhibition of cell protein synthesis, as described above.
Cells were washed twice with cold complete medium and once with PBS and dissolved in 0.1 N KOH for 10 min at 37 °C to determine the cell-associated RIP. The radioactivity was measured in a γ-counter and the results were referred to the cell number calculated as above.

Immunofluorescence and confocal microscopy

HeLa cells were seeded on cover slips into 24-well plates (3×10^4 cells/well) in complete medium. After 18 h, cells were incubated for 1 h at 0 °C with nigrin b, ricin or volkensin (5×10^{-6} M) in complete (nigrin b and volkensin) or serum-free medium (ricin), washed three times with ice-cold complete medium and incubated in complete medium at 37 °C for 15–60 min.
At the end of treatment, cells were washed three times with serum-free medium at 0 °C and fixed with 1% p-formaldehyde for 30 min at 30 °C, washed twice with PBS and permeabilized with 1% saponin for 45 min at 30 °C. After saturation with 1% BSA in PBS for 1 h at 30 °C, cells were incubated with the relevant anti-RIP antibodies and the anti-GM130 monoclonal antibody diluted 1:1000 in 1% BSA for 1 h at 30 °C, washed and stained with the FITC-conjugated anti-rabbit antibodies diluted 1:100 and the Cy5-conjugated anti-mouse antibodies diluted 1:20 in 1% BSA for 1 h at 30 °C. Finally, cover slips were mounted on glass slides using a Mowiol 4-88 solution (10% w/v) containing the anti-fade 1,4-diazobicyclo-[2.2.2]-octane (2.5% w/v) in 0.1 M Tris-HCl buffer, pH 8.5, plus glycerol (20% v/v). The multi-labelling immunofluorescence experiments were carried out avoiding cross-reactions between primary and secondary antibodies and a variety of controls were performed to ensure antibody specificity.
Confocal imaging was performed on a Radiance 2000 confocal laser scanning microscope (BioRad, Hercules, Calif.), equipped with a Nikon ×40, oil immersion 1.4 N.A. objective and with krypton and red diode lasers. For FITC and Cy5 double detection, the samples were simultaneously excited with the 488-nm line of the krypton laser and with the 637-nm line of the red diode laser. The emission signals from FITC and Cy5 were separated by a dichroic mirror (DM; 560 nm) and simultaneously detected by two photomultiplier tubes. Two barrier filters (BP; 515/30 nm for FITC and LP; 660 nm for Cy5) were placed before the two photomultiplier tubes to minimize the overlap between the two signals, as previously described [41]. Optical sections were obtained at increments of 0.3 µm in the Z-axis and were digitized with a scanning mode format of 512 × 512 pixels and 256 grey levels. Image processing and volume rendering were performed using the ImageSpace software (Molecular Dynamics, Sunnyvale, Calif.) running on a workstation Indigo (Silicon Graphics, Mountain View, Calif.).
The colocalization of the fluorochromes was evaluated by comparing the equivalent pixel positions in each of the acquired images (optical sections), using LaserPix software (BioRad). Briefly, a two-dimensional scatter plot diagram of the individual pixels from the paired images was generated. Dimmer pixels in the image were located toward the origin of the scatter plot, while brighter pixels were located farther out. Pure red and pure green pixels tended to cluster more toward the corresponding axes of the plot. If colocalized pixels were present, they appeared coloured from orange to yellow, depending on the extent of colocalization, toward the middle of the plot. For each scatter plot diagram, an area of interest was drawn on the scatter plot to indicate threshold levels of signal to be included in the analysis. Pixels with intensity values greater than 150 grey levels (on a scale from 0 to 255) were selected for both detectors, to calculate the colocalization binary maps that indicate regions containing highly colocalized signals [42]. Overlap of the signals (in yellow) corresponds to the areas of colocalization.
To evaluate the level of overlap of the signals, avoiding the typical limitations of fluorescence imaging, such as efficiency of immunoreaction, sample photobleaching and photomultiplier quantum efficiency, the coefficients k_1 and k_2 [43] were calculated on acquired optical sections. These coefficients split the value of colocalization into the two separate parameters that depend on the sum of the products of the intensities of two channels, the coefficients k_1 and k_2 being sensitive to differences in the intensity of green and red signals, respectively. Relative quantification of colocalized fluorescent signals was performed on 30 cells using overlap coefficient k_1 and was expressed as a percentage of the amount of green signal in the areas of colocalization as previously described [44]. The statistical significance of the difference between the experimental points was evaluated by Student's t test.

Results

Analysis of nigrin b- and volkensin-specific binding to HeLa cells

Nigrin b and volkensin binding to HeLa cells at saturating conditions was analysed by Scatchard plot and values of the K_d and the number of binding sites per cell were calculated and compared to those reported for ricin (fig. 1). HeLa cells showed similar numbers of receptors and K_d values for nigrin b and volkensin, which were two to three orders of magnitude lower than those reported for ricin.

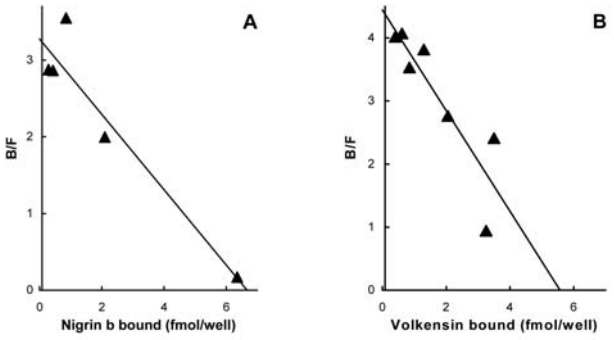

RIP	Binding sites (mol/cell)	K_d (M)
Nigrin b	2.48×10^5	8.73×10^{-11}
Ricin	3.30×10^7	3.00×10^{-8}
Volkensin	2.26×10^5	9.89×10^{-11}

Figure 1. Scatchard plots of nigrin b- and volkensin-specific binding to HeLa cells. The cells were incubated with scalar concentrations of ^{125}I-nigrin b (*A*) or ^{125}I-volkensin (*B*) for 1 h at 0 °C. Results are means of duplicate samples of one experiment. The K_d values and the numbers of binding sites were calculated by Scatchard analysis and compared to those reported for ricin binding to HeLa cells [45].

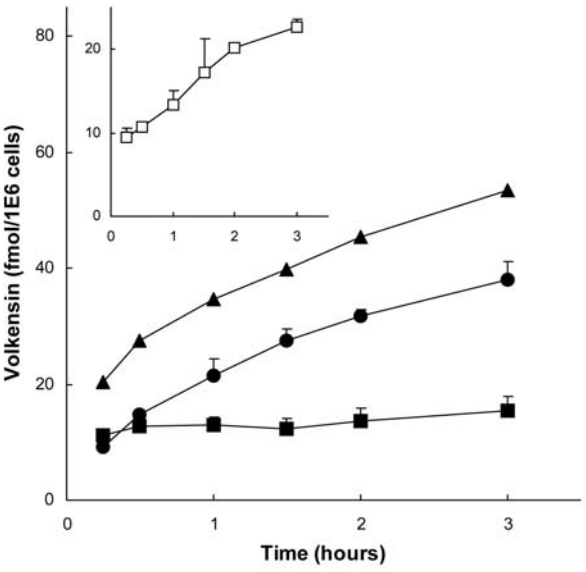

RIP	Bound	Intracellular
	fmol/10^6 cells	
Nigrin b	70.70	188.57
Ricin	763.47	2253.22
Volkensin	15.40	38.06

Figure 2. Uptake of volkensin by HeLa cells. Binding to cell membrane (■) and intracellular accumulation (●) of volkensin after incubation at 37 °C for the indicated times with 10^{-8} M ^{125}I-volkensin. Total cell-associated RIP (▲) was calculated as the sum of the intracellular and membrane-bound protein. The inset shows the binding of volkensin at 0 °C. Results are means ± SD of two experiments in duplicate samples. The amounts of membrane-bound and intracellular RIP after 3 h incubation at 37 °C were compared to corresponding nigrin b and ricin values calculated from those reported [27].

Uptake of volkensin by HeLa cells

The time-course of volkensin binding to, and uptake by, HeLa cells was investigated (fig. 2). At 0 °C, the amount of RIP bound to the cell membrane increased progressively, nearly reaching a plateau after 3 h of incubation. When cells were incubated at 37 °C, volkensin accumulated inside the cell rapidly, the intracellular amount of RIP almost matching the aliquot bound to the cell surface as early as 15 min after incubation. Moreover, cell-bound volkensin did not increase with time while total cell-associated RIP approximately doubled after 1.5 h. The amount of membrane-associated volkensin was 5- and 50-fold less, and that of intracellular volkensin 5- and 60-fold less compared with the corresponding values reported for nigrin b and ricin, respectively [27].

Intracellular localization of RIPs

To investigate the intracellular site at which anti-RIP antibodies localize, a double immunofluorescence analysis was performed with a monoclonal antibody against GM130, a cis-Golgi-associated protein involved in ER-Golgi vesicular transport. Confocal microscopy analysis showed nigrin b to be localized in discrete cytoplasmic dots (fig. 3A, E, I). Immunostaining with anti-GM130 antibody gave a fluorescent signal that was used as a marker for the Golgi apparatus (fig. 3B, F, L). The merged images, green for nigrin b and red for GM130, provided evidence that the two molecules partially colocalized at the level of the Golgi compartment (fig. 3C, G, K), as shown in detail in the insets. Colocalization was evaluated by binary maps, and was analysed in confocal microscopy, using the overlap coefficient k_1, which provides information about the differences in intensity of the green fluorescent signals on the red signals (fig. 3D, H, L). This method describes the amount of green in the areas of higher colocalization. The values of colocalization demonstrated that the maximum level of colocalization was significant (Student's t test, $p < 0.01$) within 30 min of incubation (table 1).

The immunofluorescence analysis with anti-ricin antibodies gave a signal that localized mainly in perinuclear regions, probably corresponding to ER and Golgi vesicles, as expected (fig. 4A, E, I). The colocalization analysis of ricin with GM130 (merged images presented in C, G and K, and binary maps in D, H and L) demonstrated that the signal given by ricin present in the Golgi vesicles progressively and significantly increased from 15 to 60 min of incubation.

Immunostaining with anti-volkensin antibodies resulted in a pattern very similar to that observed with ricin, although the fluorescence intensity in the perinuclear re-

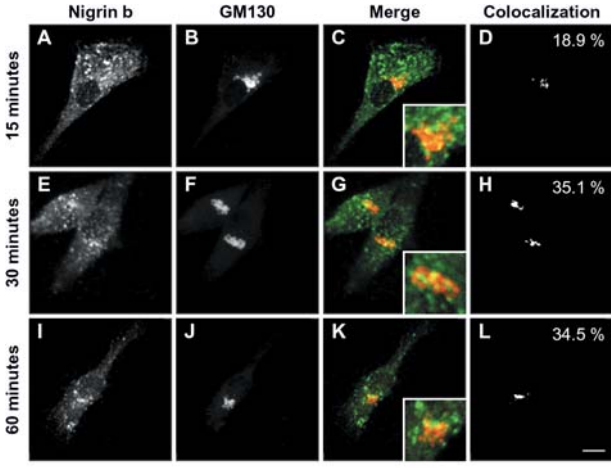

Figure 3. Double immunofluorescence analysis of nigrin b (*A, E, I*), and GM130 (B, F and J) in HeLa cells. The cells were incubated with nigrin b (5×10^{-6} M) in complete medium for 1 h at 0 °C, washed and incubated in complete medium at 37 °C for 15 (*A–D*), 30 (*E–H*) and 60 (*I–L*) min. Merged reconstructed images of extended focus projections (green for nigrin b and red for GM130) are also shown in (*C, G, H*). The insets show a detail at three times magnification. The binary maps presented in panels (*D, H, L*) give a more precise evaluation of colocalization, as they show only regions in which the two signals are present together above a defined threshold of fluorescence intensity. The values given show the amount of green signal (nigrin b) that colocalized with red signal (GM130). The values represent mean values of three different experiments expressed as percentages. Bar, 5 µm.

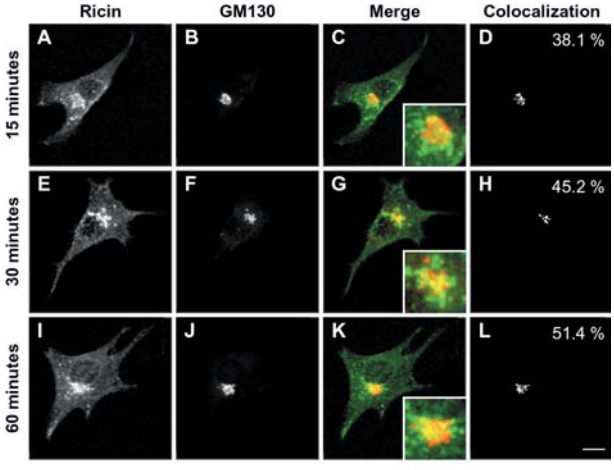

Figure 4. Double-immunofluorescence analysis of ricin (*A, E, I*), and GM130 (*B, F, J*) in HeLa cells. The cells were incubated with ricin (5×10^{-6} M) in serum-free medium for 1 h at 0 °C, washed and incubated in complete medium at 37 °C for 15 (*A–D*), 30 (*E–H*) and 60 (*I–L*) min. The panels are the same as in figure 3 except for the anti-RIP antibodies.

gions was weaker (fig. 5A, E, I). The colocalization analysis of volkensin with GM130 (merged images presented in C, G and K, and binary maps in D, H and L) show that the maximum level of colocalization was reached after 30 min of incubation and no significant differences were observed between 30 and 60 min (table 1).

Table 1. Statistical analysis (Student's t test) of overlap coefficient k_1 calculated on acquired optical sections between the colocalized fluorescent signals of anti-RIP antibodies and the anti-GM130 antibody.

	Comparison between 15 and 30 min	Comparison between 30 and 60 min
Nigrin b	p = 0.002*	p = 0.877
Ricin	p = 0.002*	p = 0.018*
Volkensin	p = 0.001*	p = 0.337

The analysis was performed comparing the different times of incubation of RIPs. The asterisk indicates a significant difference.

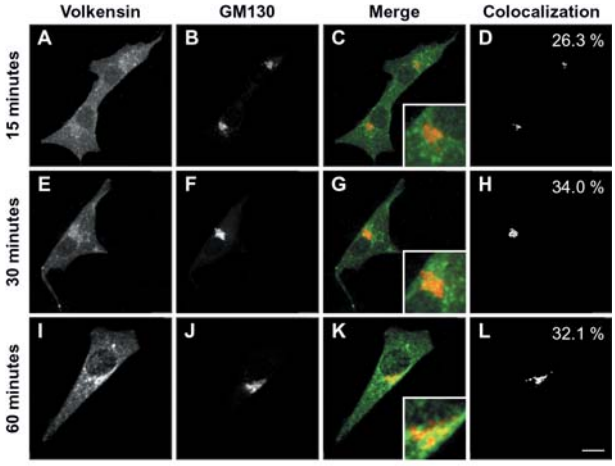

Figure 5. Double-immunofluorescence analysis of volkensin (*A, E, I*), and GM130 (*B, F, J*) in HeLa cells. The cells were incubated with volkensin (5×10^{-6} M) in complete medium for 1 h at 0 °C, washed and incubated in complete medium at 37 °C for 15 (*A–D*), 30 (*E–H*) and 60 (*I–L*) min. The panels are the same as in figure 3 except for the anti-RIP antibodies.

Inhibition of protein synthesis by HeLa cells

The inhibition of protein synthesis by HeLa cells caused by RIPs was studied in the same experimental conditions as the immunofluorescence test (fig. 6). The concentration-response curves of protein synthesis by HeLa cells after 2 h exposure to nigrin b, ricin and volkensin show the marked difference in cytotoxicity of the three RIPs (fig. 6A). Within the range of concentrations tested, only volkensin totally inhibited protein synthesis, whereas nigrin b and ricin lowered it to 39 and 23% of control cultures, respectively. The time of exposure to nigrin b required to inhibit cell protein synthesis by 50% was 2.5–3.3 times higher than that required by ricin and volkensin, respectively (fig. 6B). The effect of BFA on the inhibition of cell protein synthesis was evaluated at 1 and 2 h. The addition of BFA completely or partially protected cells from the toxic effect of volkensin or ricin, respectively, whereas no protection was observed in the case of nigrin b.

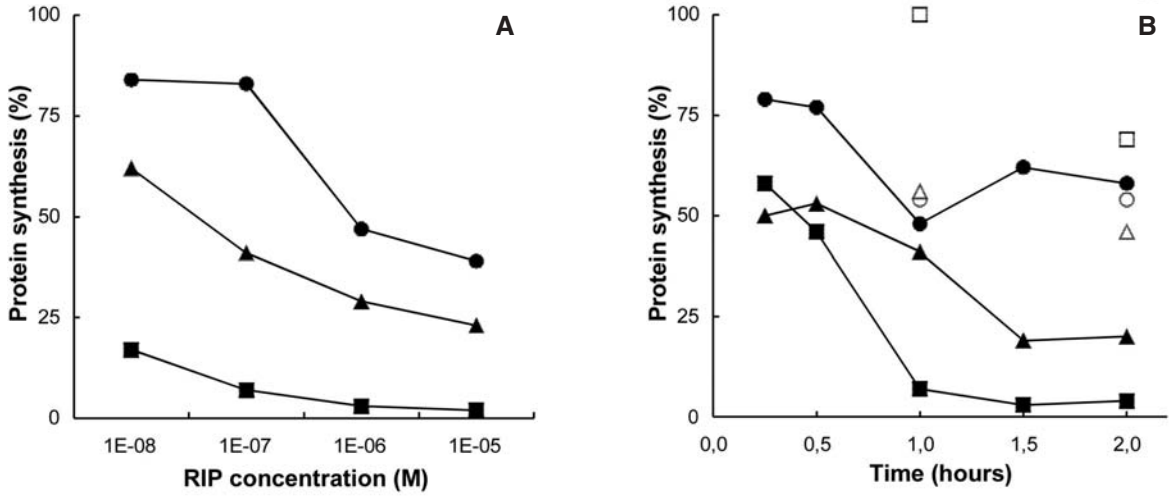

Figure 6. Inhibition of protein synthesis by RIPs. HeLa cells were incubated for 2 h with the indicated concentrations of RIPs (*A*), or for the indicated times with 5×10^{-6} M nigrin b (●), ricin (▲) or volkensin (■) in the absence or presence of (○, □, △, respectively) 5 µg/ml BFA (*B*). Protein synthesis is expressed as percentage of control cultures, which incorporated 7030 ± 1868 dpm or 4642 ± 2715 dpm, in the absence or presence of BFA, respectively. The time of exposure to RIPs required to inhibit cell protein synthesisby 50% was 88, 35 and 27 min for nigrin b, ricin and volkensin, respectively, as calculated by linear regression analysis. Results are means of duplicate or triplicate samples of one experiment.

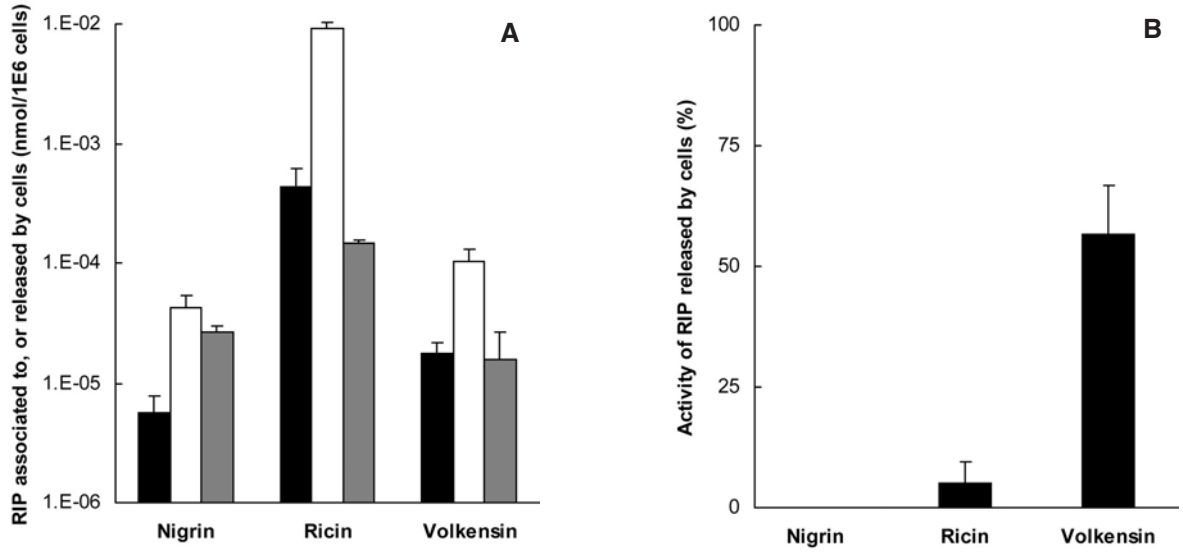

Figure 7. Exocytosis and degradation of RIPs by HeLa cells and activity of cell-released RIPs. Cells were pulsed for 1 h at 0 °C with 5×10^{-8} M ^{125}I-nigrin b, ^{125}I-ricin or ^{125}I-volkensin and washed and incubated at 37 °C in complete medium for 15–180 min. (*A*) Amount of RIP associated to cells (black column) or released by cells in the acid-soluble (white column) or acid-precipitable (grey column) fractions. The values represent the means ± SD of the amount of RIP recovered at all times from one (ricin and volkensin) or two (nigrin b) experiments in duplicate samples. The means ± SD of total RIP (cell associated and exocyted proteins) recovered at all times was 75.5 ± 10.6, 9856 ± 1104 and 136.1 ± 33.3 (fmol/10^6 cells), for nigrin b, ricin and volkensin, respectively. (*B*) Protein synthesis inhibition of RIP released by cells. Results are expressed as the percentage of the inhibition obtained with an amount of RIP equal to total cell-released RIP.

Amount and activity of RIPs released by HeLa cells

The amount and activity of RIPs released after endocytosis were evaluated in cells pulsed for 1 h at 0 °C with ^{125}I-RIPs and chased at 37 °C up to 180 min (fig. 7). After different times of incubation at 37 °C (between 15 and 180 min), almost no variation was observed in the amount of radioactivity associated with cells or in the culture medium either in the acid-precipitable or the acid-soluble fractions (results not shown).

The amounts of cell-associated and cell-released (acid-soluble plus acid-precipitable) ricin were noticeably higher than the analogous quantities of nigrin b or volkensin (fig. 7 A). Only a low percentage of the total internalized radioactivity (cell-associated plus released)

was found associated with cells, being 8, 4 and 13% for nigrin b, ricin and volkensin, respectively. Most of the radioactivity was released by cells in the acid-precipitable fraction and was 57, 94 and 75% of internalized nigrin b, ricin and volkensin, respectively. The percentage of nigrin b released by cells in the acid-soluble fraction was higher than that of ricin or volkensin (35 versus 1 and 12%, respectively).

The activity of RIPs released by cells was evaluated by the inhibition of cell protein synthesis and expressed as the percentage of the inhibitory activity of a RIP concentration corresponding to total cell-released RIP (fig. 7B). No activity was found in cell-released nigrin b. Only 5% of released ricin was active versus 57% of exocytosed volkensin.

Discussion

The present work analysed for the first time the binding to, and the uptake and degradation by, cells of volkensin, as well as its intracellular routeing and exocytosis, and compared these parameters with those of nigrin b and ricin. Our results confirm in the present experimental conditions, the higher toxicity to HeLa cells of volkensin ($IC_{50} = 3.00 \times 10^{-13}$ M [12]) compared to nigrin b and ricin ($IC_{50} = 5.36 \times 10^{-8}$ M and 1.00×10^{-12} M, respectively [27]).

The first step in the study of the interaction of volkensin with cells concerns its binding to glycosylated molecules on the cell membrane through their lectinic B chains. Scatchard analysis (fig. 1) showed that HeLa cells had comparable binding affinity and number of binding sites (2×10^5/cell) for nigrin b and volkensin, two-logs lower than those reported for ricin (1 to 3×10^7/cell [45]), and equal to those for modeccin (2×10^5/cell [46]). In comparison to ricin, a lower number of binding sites corresponded either to a lower (nigrin b) or to a greater (volkensin) toxicity to cells (fig. 1). These results indicate (i) that the higher cytotoxicity of volkensin compared to nigrin b is not caused by differences in the binding to the cell membrane and (ii) that the significantly different number of binding sites between ricin and volkensin is not associated with an equally great difference in cytotoxicity. The lack of correlation between the number of cell-binding sites for an RIP and its cytotoxicity could be explained in part by the fact that the same ligand may be routed to various subcellular compartments through binding to different receptors, which may condition the fate and the biological activity of the ligand.

Our results for volkensin binding to, and uptake by, HeLa cells (fig. 2) indicate that volkensin is rapidly taken up by cells and suggest that the receptors for this toxin on the cell surface are effective in the internalization process. These receptors must also be efficient in directing volkensin to the intracellular target, since this RIP has a higher cytotoxicity than nigrin b and ricin, despite its lower uptake. Consistent with the higher number of ricin-binding sites, HeLa cells internalized much more ricin than nigrin b or volkensin. On the other hand, the amount of nigrin b inside the cell was higher than that of volkensin, although HeLa cells have an analogous number of binding sites for each RIP. Thus, the differences in the intracellular accumulation of these RIPs can be attributed only in part to differences in the number of cell receptors. Compared with volkensin receptors, nigrin b receptors could be more efficient in ensuring endocytosis, or could be recycled more rapidly, more being available per time unit. Ricin cytotoxicity is lower than that of volkensin, although the uptake of the former is higher, indicating that the amount of cell-associated ricin is for the most part not correlated to its cytotoxicity. This consideration is consistent with the finding that only approximately 5% of the total amount of ricin within the cells reached the subcellular compartment that allows translocation to the cytosol [22]. Together, the above results suggest that there is a low correlation between (i) the level of cell binding and the uptake of RIPs and (ii) the intracellular accumulation of RIPs and their cytotoxicity.

That ricin must be delivered to the Golgi complex to exert its cytotoxic action has been known for some time [23]. Recently, the pathway followed by ricin to reach the cytosol from the Golgi through the ER has been clarified [reviewed in ref. 47]. The present work demonstrates for the first time the localization of volkensin in the Golgi stacks by morphological observations with confocal microscopy (fig. 5). Ricin and volkensin showed a very similar pattern of intracellular distribution and were clearly seen to be located mainly in the perinuclear regions. The above results were confirmed by the markedly reduced cytotoxicity of both volkensin and ricin (fig. 6A) when the transit of the RIPs through the Golgi apparatus was prevented by treating HeLa cells with BFA. This drug is known to prevent the transport of ricin to that subcellular compartment [reviewed in ref. 48]. The main difference between the internalization of volkensin and that of ricin was the progressive accumulation of ricin versus a more rapid turnover of volkensin, which reached a plateau after 30 min of incubation. The more rapid recycling of the toxin associated with a better resistance of its activity to degradation could contribute to the higher toxicity of this RIP compared to ricin. However, time-dependent interactions between toxin molecules or with the vesicular membrane could change antigenic epitope availability for polyclonal antitoxin antibodies and contribute to the different temporal pattern of ricin and volkensin colocalization in the Golgi.

Consistent with previous observations [27], BFA did not protect cells from the inhibition of protein synthesis by nigrin b, validating the hypothesis that the intracellular

routeing of this RIP is different from that confirmed for ricin and ascertained for volkensin in the present work. Indeed, nigrin b was clearly seen to be located in discrete cytoplasmic dots and only partly colocalized at the level of the Golgi compartment. Furthermore, the maximum level of colocalization of nigrin b with anti-GM130 antibody (35.1%) was obtained after 30 min of incubation at 37°C in complete medium. These data support the idea that nigrin b was degraded by cells in cytoplasmic vesicles with, as a result, lower amounts remaining, possibly already inactivated, inside the cells. Our results with confocal microscopy experiments support the conclusion that the perinuclear localization of ricin and volkensin and their high level of colocalization with the cis-Golgi structure correlate with the higher cytotoxic effect of these RIPs compared with nigrin b [49, 50].

RIP accumulation inside the cell results from a balance between endocytosis, degradation and exocytosis. Differences in degradation have been suggested to account, at least in part, for the different toxicity of nigrin b and ricin [27]. The present results show that ricin and volkensin undergo lower degradation than nigrin b, as indicated by the percentage of RIPs released by cells in the acid-soluble form (fig. 7A). Moreover, determination of the protein synthesis inhibitory activity in cell-released RIPs ascertained that 57% of volkensin and only 5% of ricin were active, while nigrin b was totally inactive (fig. 7B). Together with the low level of degradation, the higher percentage of active volkensin exocytosed by the cells explains, at least in part, its higher cytotoxicity compared to the other RIPs.

Although the proportions of cell-associated and still active cell-released ricin are low, the absolute amounts of internalized and active recyclable toxin are considerably higher than the corresponding amounts of nigrin b (fig. 7A). The amounts of cell-associated and cell-released volkensin are not substantially different from the corresponding amounts of nigrin b. However, more than 50% of the volkensin released by the cells is still active, thus being available for entering other cells (fig. 7B). The different amounts of active recyclable RIPs could be one of the reasons that volkensin has a higher toxicity than ricin and especially nigrin b not only to cells in vitro, but also to animals.

Summing up, the different intracellular routeing of the three type 2 RIPs studied here seems to be an important factor for the differences observed in their cytotoxicity. In particular, the fact that nigrin b (i) reaches the Golgi to a lower extent than ricin and volkensin, (ii) is more degraded than ricin and volkensin and (iii) is completely inactivated when exocytosed, may contribute to the low toxicity of this RIP compared with the other toxins. Although the binding to, and uptake by, cells of volkensin are lower than those of ricin, (i) the routeing to the Golgi apparatus, (ii) the rapid recycling and (iii) the higher resistance to inactivation of volkensin may contribute to its higher overall cytotoxicity. This observation may be even more important for the toxicity to animals, because the detoxification mechanism resulting from intracellular degradation may be largely missing in the case of poisoning with volkensin.

Acknowledgments. This study was supported by grants from the University of Bologna, Funds for Selected Research Topics, the Ministero dell'Istruzione, dell'Università e della Ricerca, Rome, the Ministero della Salute, Rome, the Associazione Nazionale per la Ricerca sul Cancro, Milan, the program CNR-MIUR Legge 449/97, Pallotti's Legacy for Cancer Research, the Comision Interministerial de Ciencia y Tecnologia (FIS P1030258 and BIO 98-0727) and the Consejería de Sanidad y Consumo (Junta de Castilla y León). S. Musiani was supported by a fellowship from the Fondazione Italiana per la Ricerca sul Cancro.

1 Barbieri L., Battelli M. G. and Stirpe F. (1993) Ribosome-inactivating proteins from plants. Biochim. Biophys. Acta **1154:** 237–282
2 Peumans W. J., Hao Q. and Van Damme E. J. M. (2001) Ribosome-inactivating proteins from plants: more than RNA N-glycosidases? FASEB J. **15:** 1493–1506
3 Van Damme E. J. M., Hao Q., Barre A., Vandenbussche F., Desmyter S., Rougé P. et al. (2001) Ribosome-inactivating proteins: a family of plant proteins that do more than inactivate ribosomes. Crit. Rev. Plant Sci. **20:** 395–465
4 Girbés T., Ferreras J. M., Arias F. J. and Stirpe F. (2004) Description, distribution, activity and phylogenetic relationship of ribosome-inactivating proteins in plants, fungi and bacteria. Mini-Rev. Med. Chem. **4:** 461–476
5 Endo Y. and Tsurugi K. (1986) Mechanism of action of ricin and related toxic lectins on eukaryotic ribosomes. Nucleic Acids Symp. Ser. **17:** 187–190
6 Endo Y., Mitsui K., Motizuki M. and Tsurugi K. (1987) The mechanism of action of ricin and related toxic lectins on eukaryotic ribosomes: the site and the characteristics of the modification in 28 S ribosomal RNA caused by the toxins. J. Biol. Chem. **262:** 5908–5912
7 Eiklid K., Olsnes S. and Pihl A. (1980) Entry of lethal doses of abrin, ricin and modeccin into the cytosol of HeLa cells. Exp. Cell Res. **126:** 321–326
8 Barbieri L., Valbonesi P., Bondioli M., Alvarez M. L., Dal Monte P., Landini M. P. et al. (2001) Adenine glycosylase activity in mammalian tissues: an equivalent of ribosome-inactivating proteins. FEBS Lett. **505:** 196–197
9 Walsh T. A., Morgan A. E. and Hey T. D. (1991) Characterization and molecular cloning of a proenzyme form of a ribosome-inactivating protein from maize – novel mechanism of proenzyme activation by proteolytic removal of a 2.8-kilodalton internal peptide segment. J. Biol. Chem. **266:** 23422–23427
10 Reinbothe S., Reinbothe C., Lehmann J., Becker W., Apel K. and Parthier B. (1994) JIP60, a methyl jasmonate-induced ribosome-inactivating protein involved in plant stress reactions. Proc. Natl. Acad. Sci. USA **91:** 7012–7016
11 Battelli M. G. (2004) Cytotoxicity and toxicity to animals and humans of ribosome-inactivating proteins. Mini-Rev. Med. Chem. **4:** 513–521
12 Stirpe F., Barbieri L., Abbondanza A., Falasca A. I., Brown A. N., Sandvig K. et al. (1985) Properties of volkensin, a toxic lectin from *Adenia volkensii*. J. Biol. Chem. **260:** 14589–14595
13 Sparapani M., Buonamici L., Ciani E., Battelli M. G., Ceccarelli G., Stirpe F. et al. (1997) Toxicity of ricin and volkensin, two ribosome-inactivating proteins, to microglia, astrocyte, and neuron cultures. Glia. **20:** 203–209

14 Wiley R. G. and Kline IV R. H. (2000) Neuronal lesioning with axonally transported toxins. J. Neurosci. Methods. **103:** 73–82
15 Skilleter D. N., Paine A. J. and Stirpe F. (1981) A comparison of the accumulation of ricin by hepatic parenchymal and non-parenchymal cells and its inhibition of protein synthesis. Biochim. Biophys. Acta **677:** 495–500
16 Simmons B. M., Stahl P. D. and Russell J. H. (1986) Mannose receptor-mediated uptake of ricin toxin and ricin A chain by macrophages: multiple intracellular pathways for A chain translocation. J. Biol. Chem. **261:** 7912–7920
17 Magnusson S., Kjeken R. and Berg T. (1993) Characterization of two distinct pathways of endocytosis of ricin by rat liver endothelial cells. Exp. Cell Res. **205:** 118–125
18 Girbés T., Ferreras J. M., Arias F. J., Muñoz R., Iglesias R., Jimenez P. et al. (2003) Non-toxic type 2 ribosome-inactivating proteins (RIPs) from *Sambucus*: occurrence, cellular and molecular activities and potential uses. Cell Mol. Biol. **49:** 537–554
19 Svinth M., Steighardt J., Hernandez R., Suh J. K., Kelly C., Day P. et al. (1998) Differences in cytotoxicity of native and engineered RIPs can be used to assess their ability to reach the cytoplasm. Biochem. Biophys. Res. Commun. **249:** 637–642
20 Olsnes S. and Pihl A. (1973) Different biological properties of the two constituent peptide chains of ricin, a toxic protein inhibiting protein synthesis. Biochemistry **12:** 3121–3126
21 Sandvig K. and Deurs B. van (1996) Endocytosis, intracellular transport, and cytotoxic action of Shiga toxin and ricin. Physiol. Rev. **76:** 949–966
22 Deurs B. van, Sandvig K., Petersen O. W., Olsnes S., Simons K. and Griffiths G. (1988) Estimation of the amount of internalized ricin that reaches the trans-Golgi network. J. Cell Biol. **106:** 253–267
23 Deurs B. van, Petersen O. W., Olsnes S. and Sandvig K. (1987) Delivery of internalized ricin from endosomes to cisternal Golgi elements is a discontinuous, temperature-sensitive process. Exp. Cell Res. **171:** 137–152
24 Yoshida T., Chen C. C., Zhang M. S. and Wu H. C. (1991) Disruption of the Golgi apparatus by brefeldin A inhibits the cytotoxicity of ricin, modeccin, and *Pseudomonas* toxin. Exp. Cell Res. **192:** 389–395
25 Sandvig K., Prydz K., Hansen S. H. and Deurs B. van (1991) Ricin transport in brefeldin A-treated cells: correlation between Golgi structure and toxic effect. J. Cell Biol. **115:** 971–981
26 Lord J. M. and Roberts L. N. M. (1998) Toxin entry: retrograde transport through the secretory pathway. J. Cell Biol. **140:** 733–736
27 Battelli M. G., Citores L., Buonamici L., Ferreras J. M., Benito F. M. de, Stirpe F. et al. (1997) Toxicity and cytotoxicity of nigrin b, a two-chain ribosome-inactivating protein from *Sambucus nigra*: comparison with ricin. Arch. Toxicol. **71:** 360–364
28 Battelli M. G., Barbieri L., Bolognesi A., Buonamici L., Valbonesi P., Polito L. et al. (1997) Ribosome-inactivating lectins with polynucleotide:adenosine glycosidase activity. FEBS Lett. **408:** 355–359
29 Citores L., Muñoz R., De Benito F. M., Iglesias R., Ferreras J. M. and Girbés T. (1996) Differential sensitivity of HELA cells to the type 2 ribosome-inactivating proteins ebulin l, nigrin b and nigrin f as compared with ricin. Cell. Mol. Biol. **42:** 473–476
30 Pascal J. M., Day P. J., Monzingo A. F., Ernst S. R., Robertus J. D., Iglesias R. et al. (2001) 2.8-Å crystal structure of a nontoxic type-II ribosome-inactivating protein, ebulin l. Proteins **43:** 319–326
31 Sandvig K., Sundan A. and Olsnes S. (1984) Evidence that diphtheria toxin and modeccin enter the cytosol from different vesicular compartments. J. Cell Biol. **98:** 963–970
32 Ghosh P. C. and Wu H. C. (1988) Enhancement of cytotoxicity of modeccin by nigericin in modeccin-resistant mutant cell lines. Exp. Cell Res. **174:** 397–410
33 Girbés T., Citores L., Ferreras J. M., Rojo M. A., Iglesias P. R., Muñoz R. et al. (1993) Isolation and partial characterization of nigrin b, a non-toxic novel type 2 ribosome-inactivating protein from the bark of *Sambucus nigra* L. Plant Mol. Biol. **22:** 1181–1186
34 Nicolson G. L., Blaustein J. and Etzler M. E. (1974) Characterization of two plant lectins from *Ricinus communis* and their quantitative interaction with a murine lymphoma. Biochemistry **13:** 196–204
35 Fraker P. J. and Speck J. C. Jr (1978) Protein and cell membrane iodinations with a sparingly soluble chloroamide, 1,3,4,6-tetrachloro-3a,6a-diphrenylglycoluril. Biochem. Biophys. Res. Commun. **80:** 849–857
36 Strocchi P., Barbieri L. and Stirpe F. (1992) Immunological properties of ribosome-inactivating proteins and a saporin immunotoxin. J. Immunol. Methods **155:** 57–63
37 Lowry O. H., Rosebrough N. J., Farr A. L. and Randall R. J. (1951) Protein measurement with the Folin phenol reagent. J. Biol. Chem. **193:** 265–275
38 Scatchard G. (1949) The attraction of proteins for small molecules and ions. Ann. N. Y. Acad. Sci. **51:** 660–672
39 Stirpe F., Barbieri L., Battelli M. G., Falasca A. I., Abbondanza A., Lorenzoni E. et al. (1986) Bryodin, a ribosome-inactivating protein from the roots of *Bryonia dioica* L. (white bryony). Biochem. J. **240:** 659–665
40 Battelli M. G., Polito L., Bolognesi A., Lafleur L., Fradet Y. and Stirpe F. (1996) Toxicity of ribosome-inactivating proteins containing immunotoxins to a human bladder carcinoma cell line. Int. J. Cancer **65:** 485–490
41 Riccio M., Di Giaimo R., Pianetti S., Palmieri P. P., Melli M. and Santi S. (2001) Nuclear localization of cystatin B, the cathepsin inhibitor implicated in myoclonus epilepsy (EPM1). Exp. Cell Res. **262:** 84–94
42 Tabellini G., Bortul R., Santi S., Riccio M., Baldini G., Cappellini A. et al. (2003) Diacylglycerol kinase-θ is localized in the speckle domains of the nucleus. Exp. Cell Res. **287:** 143–154
43 Manders E. M. M., Verbeek F. J. and Aten A. (1993) Measurement of co-localization of object in dual-colour confocal images. J. Microsc. **169:** 375–382
44 Riccio M., Dembic M., Cinti C. and Santi S. (2004) Multifluorescence labeling and colocalization analyses. In: methods in Molecular Biology: Cell Cycle Control and Dysregulation Protocols, Giordano A. and Romano G. (eds), Humana, New York, pp. 171–177
45 Sandvig K., Olsnes S. and Pihl A. (1976) Kinetics of binding of the toxic lectins abrin and ricin to surface receptors of human cells. J. Biol. Chem. **251:** 3977–3984
46 Olsnes S., Sandvig K., Eiklid K. and Pihl A. (1978) Properties and action mechanism of the toxic lectin modeccin: interaction with cell lines resistant to modeccin, abrin, and ricin. J. Supramol. Struct. **9:** 15–25
47 Sandvig K., Grimmer S., Lauvrak S. U., Torgersen M. L., Skretting G., Deurs B. van et al. (2002). Pathways followed by ricin and Shiga toxin into cells. Histochem. Cell Biol. **117:** 131–141
48 Wesche J. (2002) Retrograde transport of ricin. Int. J. Med. Microbiol. **291:** 517–521
49 Iversen T. G., Skretting G., Llorente A., Nicoziani P., Deurs B van. and Sandvig K. (2001) Endosome to Golgi transport of ricin is independent of clathrin and of the Rab9- and Rab11-GTPases. Mol. Biol. Cell. **12:** 2099–2107
50 Lauvrak S. U., Llorente A., Iversen T. G. and Sandvig K. (2002) Selective regulation of the Rab9-independent transport of ricin to the Golgi apparatus by calcium. J. Cell Sci. **115:** 3449–3456